Geophysical Research Letters®

Correspondence to:

A. Booth,
A.Booth@soton.ac.uk

Ice Sheet-Albedo Feedback Estimated From Most Recent Deglaciation

Alice Booth[1] , Philip Goodwin[1] , and B. B. Cael[2]

[1]School of Ocean and Earth Science, University of Southampton, Southampton, UK, [2]National Oceanography Centre, Southampton, UK

Abstract Ice sheet feedbacks are underrepresented in model assessments of climate sensitivity and their magnitudes are still poorly constrained. We combine a recently published record of Earth's Energy Imbalance (EEI) with existing reconstructions of temperature, atmospheric composition, and sea level to estimate both the magnitude and timescale of the ice sheet-albedo feedback since the Last Glacial Maximum. This facilitates the first opportunity to quantify this feedback over the most recent deglaciation using a proxy data-driven approach. We find the ice sheet-albedo feedback to be amplifying, increasing the total climate feedback parameter by 42% and reaching an equilibrium magnitude of 0.55 $Wm^{-2}K^{-1}$, with a 66% confidence interval of 0.45–0.63 $Wm^{-2}K^{-1}$. The timescale to equilibrium is estimated as 3.6 ka (66% confidence: 1.9–5.5 ka). These results provide new evidence for the timescale and magnitude of the amplifying ice sheet-albedo feedback that will drive anthropogenic warming for millennia to come.

Plain Language Summary During a deglacial transition, ice sheets melt and retreat, decreasing the reflectivity of the land surface and increasing the surface temperature, leading to further melting. It is agreed that this feedback amplifies global warming on millennial timescales, but the exact magnitude and timescale are still very uncertain. This is important because the stronger the feedback, the more sensitive Earth's climate is to carbon dioxide on long timescales. We use proxy data records of the past 25,000 years to quantify the ice sheet-albedo feedback since the Last Glacial Maximum and estimate the time taken for the feedback to reach equilibrium and stabilize. We find that the ice sheet-albedo feedback strongly amplifies warming over thousands of years, increasing our understanding of how human activity today will continue to influence our climate for generations into the future.

1. Introduction

Constraining the magnitude of Earth's climate feedbacks has been a high priority for the scientific community in recent years to ensure that our predictions of future climate change are well-informed by accurate estimates of Earth's climate sensitivity. However, slow feedbacks that operate on timescales of more than a century continue to be overlooked in favor of near-term climate impacts. This limits our full understanding of the Earth System and how it may be affected by anthropogenic activity for far longer than a human lifetime (Clark et al., 2016). Ice sheet extent has a considerable influence on the climate on timescales of centuries to millennia, primarily through direct changes to land albedo and indirectly through the alteration of cloud cover over the northern Atlantic and Pacific Oceans (Abe-Ouchi et al., 2015; Cooper et al., 2024; Fyke et al., 2018; Vizcaíno et al., 2008; Zhu & Poulsen, 2021). The IPCC Sixth Assessment Report states with high confidence that it is *'very likely'* that the ice sheet-albedo feedback has an amplifying effect on millennial timescales, but the specific magnitude or exact response timescale is very uncertain (Forster et al., 2021).

As many global climate models are primarily used to predict climate change over the next one to two centuries, ice sheet-climate interactions are often simplified as their influence on climate sensitivity is assumed to be insignificant on these short timescales (Madsen et al., 2022). Fast feedbacks arising from small-scale changes in snow albedo are well represented in global climate models (GCMs) with understanding based on observational data (Box et al., 2012; Fyke et al., 2018; Ryan et al., 2019). However, on longer timescales, the integration of large-scale changes to ice sheet-albedo into a GCM is challenging and no GCM includes a two-way coupled dynamical ice sheet component (e.g., (Schmidt et al., 2023; R. Smith, George and Gregory, 2021)). When using the deglaciation to estimate present-day climate sensitivity, ice sheet-climate interactions are commonly included as a source of radiative forcing rather than as a feedback mechanism (Rohling, Sluijs, et al., 2012).

The challenge of quantifying the ice sheet-albedo feedback stems from an ongoing struggle to reconstruct ice sheet extent with sufficient temporal resolution and disentangle the relationship between global surface temperatures, ocean heat content, and ice sheet retreat in proxy records (Elderfield et al., 2012; Rohling et al., 2021; Shakun et al., 2015). However, a newly published proxy-based record for Earth's Energy Imbalance (EEI (Shackleton et al., 2023):) since the Last Glacial Maximum (LGM) now allows the calculation of the time evolution of the climate feedback parameter, λ, over the last deglaciation both with and without the ice sheet-albedo feedback included. This progress comes from combining existing reconstructions of surface temperature, atmospheric composition and the albedo effect of changes in ice sheet extent reflected in sea level reconstructions.

This study represents a novel attempt to simultaneously constrain the ice sheet-albedo feedback magnitude and response timescale based on proxy-based evidence and without the need for model-based assumptions of the time evolution of energy imbalance. Earth's most recent deglaciation (∼19–7 ka before present (BP)) offers a unique opportunity to study ice sheet-climate interactions as the period saw the dramatic collapse of the Laurentide and Eurasian ice sheets and a subsequent rise in global sea level by ∼120 m (Lambeck et al., 2014; Lecavalier et al., 2014; Quiquet et al., 2021; Simms et al., 2019). Global mean surface temperatures increased by approximately 7°C from the onset of the deglaciation to the preindustrial period and this relatively rapid change in temperature provides an excellent testing ground in which to explore climate feedback behavior (Kaufman et al., 2020; Osman et al., 2021; Snyder, 2016).

2. Materials and Methods

The total climate feedback parameter, λ_{total}, is the additive combination of j internal feedbacks, $\sum \Delta \lambda_j$, and can be calculated using Earth's most recent deglaciation according to the traditional linear energy budget equation:

$$\lambda_{total} = \frac{\Delta N - \Delta F_{total}}{\Delta T} \tag{1}$$

where λ_{total} is the total effective climate feedback parameter ($Wm^{-2}K^{-1}$), and takes the sign convention that λ_{total} is negative for a stable climate system, such that individual amplifying feedbacks are positive contributions to λ_{total} and individual damping feedbacks are negative contributions to λ_{total}; ΔN is the net top-of-atmosphere (TOA) energy imbalance anomaly (also referred to as EEI, Wm^{-2}); ΔF_{total} is the sum of i external forcings, $\sum \Delta F_i$, and is therefore the total radiative forcing anomaly (Wm^{-2}); and ΔT is the global surface temperature anomaly (K), all relative to the LGM. The energy imbalance from ice sheet-albedo (Wm^{-2}) can be included in the above energy budget equation in two possible ways: either as F_{alb} and part of the external forcings, $\sum \Delta F_i$, or as λ_{alb} and part of the internal feedbacks, $\sum \Delta \lambda_j$ (e.g., Rohling, Sluijs, et al. (2012)). We calculate the magnitude of λ_{total} using both methods.

In either case, the influence of the ice sheet-albedo feedback on spatial patterns of temperature change should not be ignored (Cooper et al., 2024). The total ice sheet feedback is the additive combination of direct and indirect effects on the climate system, but the radiative contribution from indirect pattern effects resulting from changes to ice sheet extent is very difficult to quantify. Therefore, we specifically target the direct influence of albedo change from ice sheet retreat in this study and apply a later adjustment to account for indirect pattern effects. With the time-evolving estimate of λ_{total} that we calculate here, we can constrain the magnitude of the ice sheet-albedo feedback at equilibrium, $\lambda_{alb(\infty)}$, and its timescale.

The recent record for EEI over the last deglaciation by Shackleton et al. (2023) based on benthic foraminiferal $\delta^{18}O$ data is utilized here to represent a novel proxy-based estimate and uncertainty of ΔN in the above Equation 1. ΔT is here calculated from Osman et al. (2021) who used model simulations and palaeoclimate proxy data to assimilate a globally resolved record of surface temperature change for the past 24 ka (Osman et al., 2021). ΔF_{total} is comprised of instantaneous radiative forcing records for CO_2, CH_4, and N_2O (greenhouse gases: GHGs) from Köhler et al. (2017), atmospheric dust, and ice sheet-albedo change since the LGM. Radiative forcing from atmospheric dust is calculated from the Lambert et al. (2012) dust flux record, which used high resolution ice core data from EPICA Dome C, Antarctica, and is converted using a linear scaling following Rohling, Medina-Elizalde, et al. (2012):

$$\Delta F_{dust} = -1.9 \log_{10}(\Delta\chi) \qquad (2)$$

where $\Delta\chi$ is the change in dust flux (Lambert et al., 2012; Rohling, Medina-Elizalde, et al., 2012). An additional $\pm50\%$ uncertainty was applied to the dust forcing calculation following Rohling, Medina-Elizalde, et al. (2012) to reflect uncertainty in the relationship between measured quantities and climate forcing. Meanwhile, radiative forcing from ice sheet-albedo change since the LGM is calculated following Rohling, Medina-Elizalde, et al. (2012) and Hansen et al. (2008) who established a linear relationship between sea level change, ΔSL (in meters), and subsequent forcing impact in ΔF_{alb} (in Wm^{-2}):

$$\Delta F_{alb} = 0.0308\Delta SL \qquad (3)$$

where ΔSL is negative during glacial periods (Hansen, 2008; Rohling, Medina-Elizalde, et al., 2012). An additional $\pm20\%$ uncertainty is applied to the calculation of ice sheet-albedo forcing, ΔF_{alb}, following Rohling, Medina-Elizalde, et al. (2012). Sea level data is sourced from Lambeck et al. (2014) who reconstruct global sea level and ice volumes since the LGM (Lambeck et al., 2014). All best estimates and standard deviations are interpolated to an annual temporal frequency for the past 25 ka to capture the LGM and subsequent deglaciation. In the case of ΔF_{dust}, the annual record is smoothed with a 501-year smoothing spline to extract the long-term signal and reduce the influence of random noise. As the focus of this study is the estimation of λ_{total} over the most recent deglaciation, all records are made relative to 18 ka BP to reflect the point at which global temperatures started to increase.

In order to quantify uncertainty, 5,000 estimates for λ_{total} are generated, with a different random number coefficient on a normal distribution, N (0,1), for each variable in the energy budget equation (CO_2, N_2O, CH_4, dust, and ice sheet albedo forcing, temperature, and EEI) and each simulation. These coefficients are then applied to each simulation as a multiplier on the standard deviation across all 18,001 timesteps of each simulation. In this way, a probability distribution of possible values can be generated for each variable, including λ_{total}.

Figure 1a compares the change in combined radiative forcing from CO_2, CH_4, and N_2O (GHGs) and dust over the past 18 ka to the change in radiative forcing from GHGs, dust and ice sheet-albedo. When ice sheet-albedo forcing is excluded from forcing, the increase in combined forcing increases steadily, before stabilizing around 11 ka BP at 5.0 ± 0.5 Wm^{-2}, coinciding with the early Holocene (Figure 1a: blue). A small decrease to 4.1 ± 0.2 Wm^{-2} at 6.5 ka BP is followed by a gentle increase to 5.1 ± 0.4 Wm^{-2} by 3 ka BP and then the sharp rise in the industrial period. This contrasts with the pink curve, which includes the added influence of radiative forcing from ice sheet-albedo change. In this case, total forcing quickly exceeds 5 Wm^{-2} by 13.5 ka BP and maintains an increasing trend throughout the Holocene to stabilize at approximately 8.8 ± 0.8 Wm^{-2} in the most recent three millennia before the familiar rapid rise in the industrial period (Figure 1a: pink). This illustrates the notable influence of ice sheet-albedo change on global total radiative forcing over time. The treatment of ice sheet-albedo change as a forcing necessitates the inclusion of ΔF_{alb}, which introduces approximately 1 Wm^{-2} of additional uncertainty by the end of the simulated period (Figure 1a: pink). This highlights the need for more precise records of ice volume change over time as well as improved understanding of the relationship between ice volume and effective radiative forcing from ice sheet changes (Zhu & Poulsen, 2021). We assume that orbital changes in the amount of solar radiation received by the Earth are significantly smaller than this forcing and so are not included in this analysis (Beer et al., 2000; Lisiecki, 2010; Rial et al., 2013).

The radiative forcing contribution from ice sheet-albedo change is better illustrated in Figure 1b which depicts the difference between the two curves in Figure 1a. The total change in radiative forcing from ice sheet retreat (ΔF_{alb}) continuously increases after 18 ka BP until it stabilizes at approximately 3.7 ± 0.4 Wm^{-2} by 6 ka BP, according to the proxy record. This value is within the uncertainty range of -3.2 Wm^{-2} of effective radiative forcing (ERF) from land ice sheets at the LGM, estimated by Zhu and Poulsen (2021), lending some confidence to the model used in this study. It should be noted that the calculation of ERF also accounts for ice sheet-climate interactions with the atmospheric temperature profile, water vapor, and clouds, and this contribution should ideally be considered. However, at the time of writing we, the authors, are not aware of the existence of any high resolution, transient record for ERF from GHGs, dust, or ice sheet-albedo over the course of the last deglaciation. Therefore, all references to radiative forcing data in this study refer to instantaneous radiative forcing (IRF), as opposed to
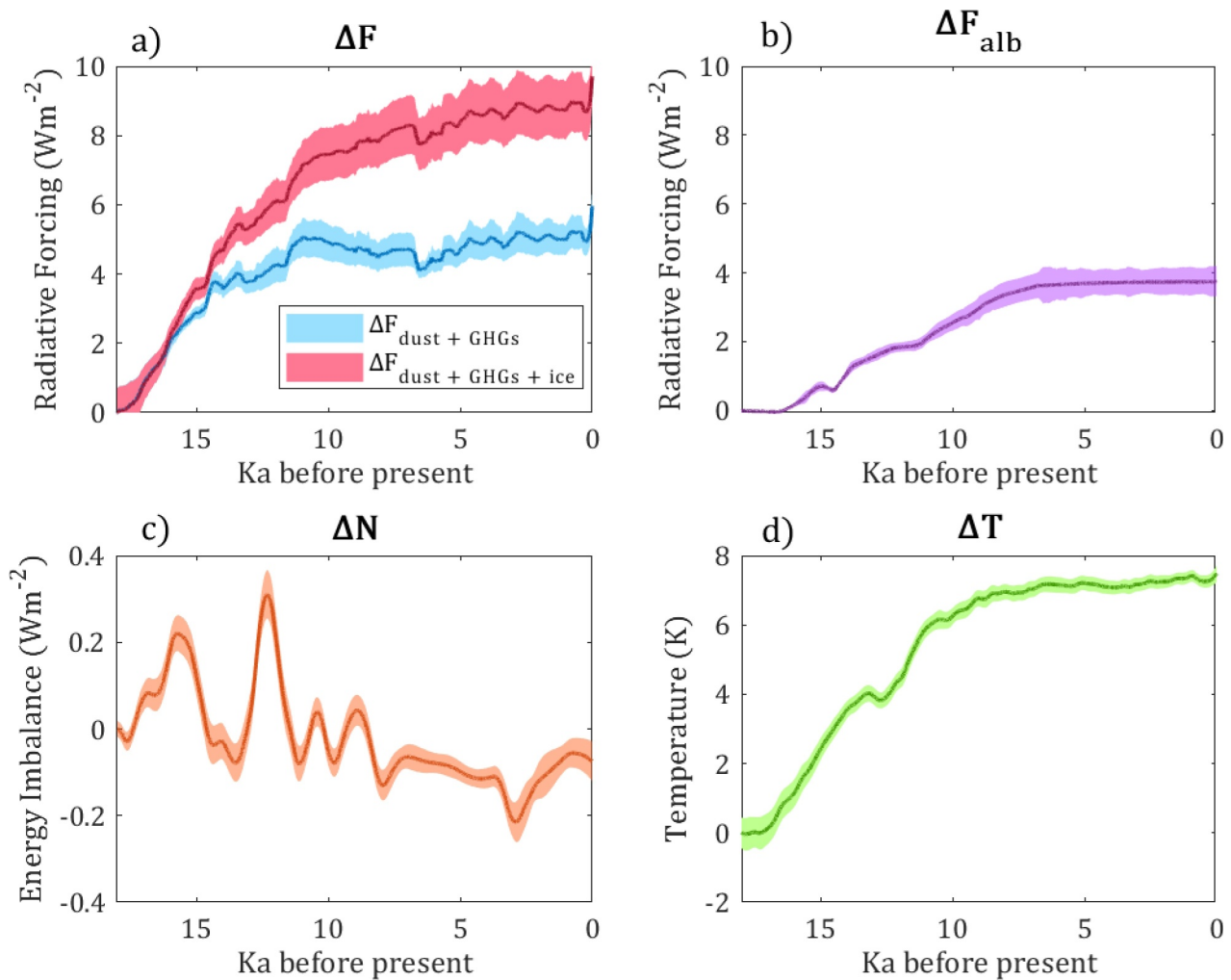
Figure 1. The components of the energy budget equation over the past 18 ka with 1σ uncertainty (shaded areas). All plots are displayed as anomalies relative to 18 ka BP (a) Change in total radiative forcing when forcing from ice sheet-albedo change is included (pink) and excluded (blue) (b) Change in total radiative forcing from ice sheet-albedo change, (c) Change in Earth's Energy Imbalance, (d) Global surface temperature anomaly.

ERF which is the preferred measure used in assessments of modern climate sensitivity (Forster et al., 2016, 2021; Smith et al., 2020).

Figure 1c depicts the change in Earth's TOA energy imbalance over time, as adapted from Shackleton et al. (2023). There is substantial fluctuation over the past 18 ka, but the overall trend is that of a gentle decrease in EEI over the simulated period, which would indicate that the warming trend since the deglaciation is unforced by changes in the energy budget. Finally, Figure 1d shows the global mean surface temperature anomaly since the deglaciation. We see approximately 7.5 K of warming over the past 18 ka, although most of this warming took place in the first 10 ka. The small dip at 12.7 ka BP represents the Younger Dryas cold period, the most recent and most severe stadial since the LGM. The return to the warming trend coincides with a spike in EEI and a sharp rise in total radiative forcing, highlighting good temporal agreement between proxy data sets.

To estimate the magnitude of the millennial scale ice sheet-albedo feedback, λ_{total} is calculated in two different ways: by considering ice sheet-albedo change as a forcing rather than a feedback, and therefore included in ΔF_{total} (Equation 1), or as a feedback rather than a forcing and so ice sheet-albedo change is excluded from ΔF_{total}. The difference between these two estimates represents the ice sheet-albedo feedback, λ_{alb}, and is calculated for all timesteps in all 5,000 simulations. The initial 1.5 ka are excluded from analysis as, during this interval, ΔT remains very close to zero, causing numerical instability (Equation 1) and is too small to provide a reliable estimate for λ.

In order to identify the timescale of the feedback, λ_{alb} is applied to a non-linear regression model according to:

$$\lambda_{alb} = \lambda_{alb^{(\infty)}}\left(1 - e^{-t/\tau}\right) \tag{4}$$

Where λ_{alb} is the estimate of the ice sheet-albedo feedback at timestep, t, and $\lambda_{alb^{(\infty)}}$ is the magnitude of the ice sheet-albedo feedback at equilibrium. τ is the response timescale that λ_{alb} operates over, that is the time taken to reach equilibrium. The above regression model is applied to all 5,000 simulations to generate 5,000 estimates for $\lambda_{alb^{(\infty)}}$ and τ, which are subsequently analyzed. Standard error weighting is found to have no significant impact on the probability distributions for each variable, so it is not used for our main analysis. By its nature, the above equation can yield numerical instabilities where values near very close to zero. Such outliers are removed from the overall ensemble of estimates to prevent erroneous bias. An outlier is defined here as being three or more scaled Median Absolute Deviations from the median.

Finally, we consider how ice sheets influence other feedbacks by altering the spatial pattern of temperature change, utilizing proxy-derived estimates from Cooper et al. (2024) as a modification applied post-analysis. The total ice sheet feedback, $\lambda_{ice\ sheets}$, is therefore represented by the following equation:

$$\lambda_{ice\ sheets} = \lambda_{alb} + \lambda' \tag{5}$$

where λ' represents the modification to the total feedback resulting from indirect pattern effects. λ' increases the total ice sheet feedback, $\lambda_{icesheets}$, by N (0.37,0.23) $Wm^{-2}K^{-1}$ (Cooper et al., 2024).

3. Results

Figure 2a shows the total climate feedback parameter, λ_{total}, when ice sheet-albedo change is treated as a forcing (pink) or feedback (blue). Prior to 16 ka, there is little difference between the magnitude of λ_{total} of either simulation, each peaking at approximately $-1.7\ Wm^{-2}K^{-1}$ and $-1.6\ Wm^{-2}K^{-1}$ respectively, supporting the notion that the ice sheet-albedo feedback was small on short timescales, although uncertainty is large. Over the course of the deglaciation, the two simulations diverge due to the influence of the ice sheet-albedo feedback. However, the evolution of λ_{total} follows a similar overall trend in either case; both increase steadily until ~6.5 ka BP, before gently decreasing again and stabilizing by ~2.5 ka BP. When ice sheet-albedo change is included as a forcing, λ_{total} stabilizes at approximately $-1.2 \pm 0.1\ Wm^{-2}K^{-1}$. When ice sheet-albedo change is included as a feedback, λ_{total} stabilizes at $-0.7 \pm 0.07\ Wm^{-2}K^{-1}$ in the final 2.5 ka BP.

The difference between the value of λ_{total} when ice sheet-albedo change is treated as either a forcing or feedback gives the climate feedback contribution from ice sheet-albedo change, λ_{alb}, which is displayed over time in Figure 2b. There is some fluctuation over time, but the overall trend closes to equilibrium after O (10,000) years. Figure 2b also shows the influence of indirect spatial pattern effects: applying the estimates from Cooper et al. (2024) in the form of the modification, λ', results in a mean increase of 67% in the total ice sheet feedback, $\lambda_{alb} + \lambda'$ (gray), compared to the ice sheet-albedo feedback, λ_{alb}, alone (purple). However, the influence of indirect pattern effects from ice sheets is still poorly constrained, and this is highlighted in the substantial additional uncertainty applied to the estimate of the total ice sheet feedback, $\lambda_{alb} + \lambda'$, compared to the estimated magnitude of the ice sheet-albedo feedback, λ_{alb}.

The impact of the ice sheet-albedo feedback, λ_{alb}, on the total climate feedback, λ_{total}, over time is further illustrated in Figure 2c which expresses the percentage change in λ_{total} when λ_{alb} is included in the estimate. As λ_{alb} progresses to equilibrium, its contribution to the magnitude of λ_{total} increases substantially. By the late Holocene (5 ka BP to present), the ice sheet-albedo feedback increases the total climate feedback parameter by 42% on average.

The probability distribution of the ice sheet-albedo feedback, λ_{alb}, is depicted in Figure 3a which shows a best estimate 0.55 $Wm^{-2}K^{-1}$ with a 66% confidence interval of 0.45–0.63 $Wm^{-2}K^{-1}$ and 95% confidence interval of 0.33–0.77 $Wm^{-2}K^{-1}$. This represents an amplifying effect, which becomes even larger if the influence of the ice sheets on temperature patterns and nonlocal feedbacks is accounted for, as shown by the gray range. Figure 3b, meanwhile, shows the probability distribution of the response timescale, τ, of the ice sheet-albedo feedback,
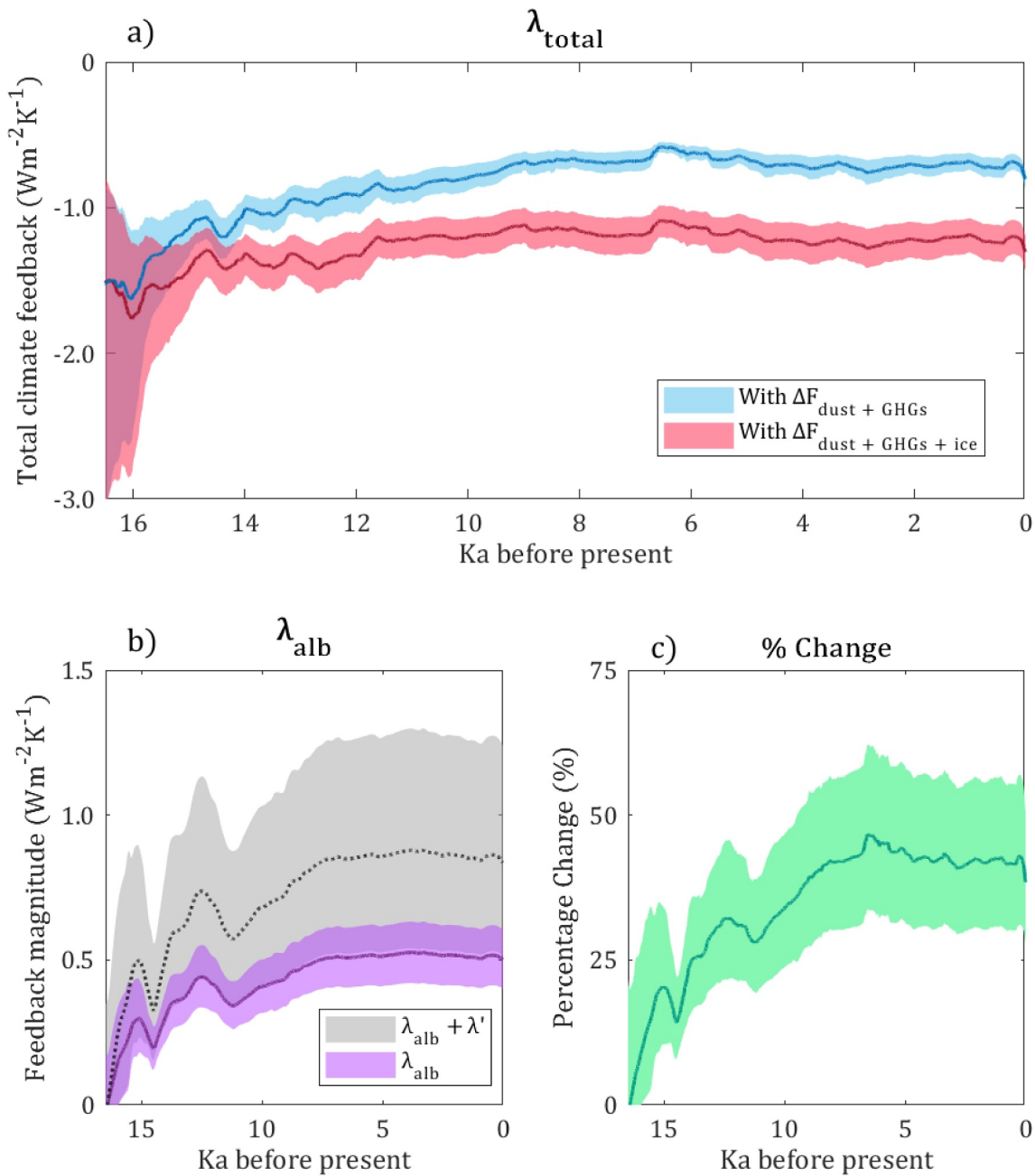
Figure 2. The magnitude of the effective climate feedback parameter, λ, over the past 16.5 ka with 66% confidence interval shaded (a) total climate feedback parameter, λ_{total}, when ice sheet-albedo is assumed to be a forcing (pink) or feedback (blue), (b) ice sheet-albedo feedback, λ_{alb} (purple) and with pattern effect (gray), (c) impact of the ice sheet-albedo feedback, λ_{alb}, on the total climate feedback parameter, λ_{total}, expressed as a percentage change.

meaning the time taken for the feedback to reach equilibrium following a perturbation. We find a best estimate for τ of 3.6 ka, with a 66% confidence interval of 1.9 to 5.5 ka. The 95% confidence interval of 0.5 to 9.3 ka reveals a positive skew toward longer timescales.

4. Discussion and Conclusions

The primary aim of this study was to constrain both the magnitude and response timescale of Earth's ice sheet-albedo feedback using proxy records of the last deglaciation. We find that λ_{alb} has a 66% confidence interval of 0.45–0.63 $Wm^{-2}K^{-1}$, with a best estimate of 0.55 $Wm^{-2}K^{-1}$ (Figure 3a). The feedback has a 95% confidence

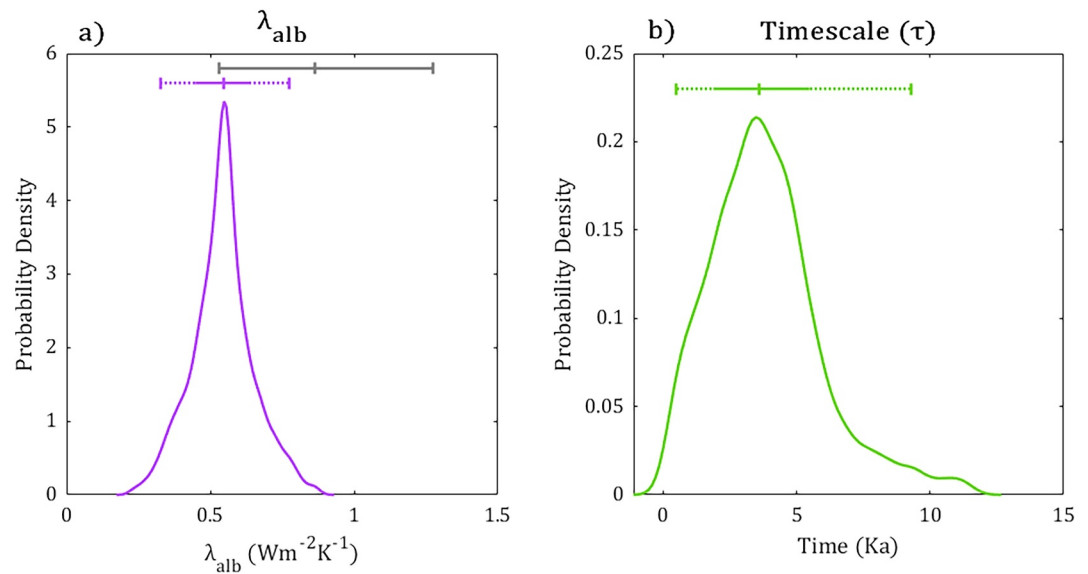**Figure 3.** Probability density distributions for (a) ice sheet-albedo feedback, λ_{alb}, and (b) the response timescale, τ, for λ_{alb}. Uncertainty intervals are displayed above each graph. Solid line indicates '66% confidence interval, dotted line indicates 95% confidence interval. The best estimate and 66% confidence interval for $\lambda_{alb} + \lambda'$ is given by the gray solid line for comparison (Figure 3a).

interval of 0.33–0.77 $Wm^{-2}K^{-1}$ supporting previous work that finds that ice sheet-albedo change has an amplifying effect. Furthermore, we find that the inclusion of the ice sheet-albedo feedback increases the total climate feedback parameter by approximately 42% at equilibrium, providing increased confidence that the amplifying effect of ice sheet retreat is not negligible. This effect becomes even stronger when the additional impact on spatial temperature patterns and nonlocal feedbacks are considered, increasing the best estimate of the total ice sheet feedback to 0.86 $Wm^{-2}K^{-1}$ with a 66% confidence interval of 0.53–1.28 $Wm^{-2}K^{-1}$. Indeed, considerable uncertainty persists around the quantification of the pattern effects resulting from changing ice sheet extent and the inclusion of a modification to account for them in this analysis substantially widens the estimated range. They are however a vital component in the interaction between ice sheets and the wider climate system and further work to increase understanding and improve quantification is required.

Additionally, we find with 66% confidence that λ_{alb} operates on a timescale of 1.9 to 5.5 ka, with a best estimate of 3.61 ka (Figure 3b). However, the 95% confidence interval of 0.5 to 9.3 ka indicates that considerable uncertainty remains surrounding the exact response timescale of the ice sheet-albedo feedback. This is a limitation of using a single time interval of only 18 ka and certainty could be increased by repeating this experiment using multiple glacial cycles, although the limited availability of long, high resolution proxy records for radiative forcing and EEI may make this challenging with additional uncertainty introduced.

This timescale estimate is applicable to a deglacial transition where ice sheets are experiencing shrinkage. The timescale over which ice sheets grow during a glacial transition and subsequently influence Earth's temperature, are subject to different physical processes and the feedback will behave differently. Furthermore, these findings specifically measure the magnitude of the ice sheet-albedo feedback for the most recent deglaciation. This is important to note as the initial ice sheet extent will differ for other periods of deglaciation. Indeed, the amplifying effect of future ice sheet retreat is likely to be comparatively reduced as the present extent of the Greenland ice sheet is smaller than that of the Laurentide ice sheet. However, ice sheet changes over Antarctica were minimal during the most recent deglaciation, and these could become substantial in the future, contributing to an amplifying ice sheet-albedo feedback regardless of the extent of the northern hemisphere ice sheets. Future work to estimate the ice sheet-albedo feedback using other glaciations and deglaciations in Earth's history could provide interesting insights as more data on these distant palaeoclimate periods is collected. Additionally, this area of research would benefit from a full quantification of ERF and transient pattern effects over the most recent deglaciation to increase the accuracy of estimates of radiative forcing from ice sheet-climate interactions.

This finding has implications for climate sensitivity and the role of ice sheet-climate interactions on long timescales. It is important to reiterate that the climate response to forcing is not constant in time, and instead climate sensitivity and climate feedbacks evolve over time in response to complex interactions between multiple forcings and feedbacks (Cael et al., 2022, 2023; Goodwin, 2018; Rohling et al., 2018; Zeebe, 2013). Although the ice sheet-albedo feedback will have a negligible influence on climate sensitivity and warming in the 21st century, its influence is substantial on millennial timescales which could have a substantial impact on all components of the Earth System, particularly the biosphere (Bao et al., 2021; Cabré et al., 2015; Lenton et al., 2006; Spencer & Christy, 2023; Stone & Lunt, 2013; Willeit et al., 2014). This highlights the importance of accounting for slow climate feedbacks like that of ice sheet-albedo change in evaluations of climate sensitivity (Cooper et al., 2024) as well as the value of measures like Earth System Sensitivity that take these processes into account (Clark et al., 2016; Golledge et al., 2019; Knutti & Rugenstein, 2015; Knutti et al., 2017; Lunt et al., 2010). Finally, these findings further highlight the increasing urgency for an effective climate change mitigation strategy to avoid serious long-term consequences for our planet and its ecosystems.

Data Availability Statement

All data is available from published works. Dust flux record is available through Lambert et al. (2012); sea level data is available from the supplementary material of Lambeck et al. (2014); radiative forcing from greenhouse gases is available from Köhler et al. (2017); temperature data is available from Osman et al. (2021); and EEI record available from Shackleton et al. (2023).

References

Abe-Ouchi, A., Saito, F., Kageyama, M., Braconnot, P., Harrison, S. P., Lambeck, K., et al. (2015). Ice-sheet configuration in the CMIP5/PMIP3 last glacial maximum experiments. *Geoscientific Model Development*, 8(11), 3621–3637. https://doi.org/10.5194/gmd-8-3621-2015

Bao, Z., Zhang, J., Wang, G., Guan, T., Jin, J., Liu, Y., et al. (2021). The sensitivity of vegetation cover to climate change in multiple climatic zones using machine learning algorithms. *Ecological Indicators*, 124, 107443. https://doi.org/10.1016/j.ecolind.2021.107443

Beer, J., Mende, W., & Stellmacher, R. (2000). The role of the sun in climate forcing. *Quaternary Science Reviews*, 19(1), 403–415. https://doi.org/10.1016/s0277-3791(99)00072-4

Box, J. E., Fettweis, X., Stroeve, J. C., Tedesco, M., Hall, D. K., & Steffen, K. (2012). Greenland ice sheet albedo feedback: Thermodynamics and atmospheric drivers. *The Cryosphere*, 6(4), 821–839. https://doi.org/10.5194/tc-6-821-2012

Cabré, A., Marinov, I., & Leung, S. (2015). Consistent global responses of marine ecosystems to future climate change across the IPCC AR5 earth system models. *Climate Dynamics*, 45(5), 1253–1280. https://doi.org/10.1007/s00382-014-2374-3

Cael, B. B., Bloch-Johnson, J., Ceppi, P., Fredriksen, H. B., Goodwin, P., Gregory, J. M., et al. (2023). Energy budget diagnosis of changing climate feedback. *Science Advances*, 9(16), eadf9302. https://doi.org/10.1126/sciadv.adf9302

Cael, B. B., Britten, G. L., Mir Calafat, F., Bloch-Johnson, J., Stainforth, D., & Goodwin, P. (2022). Climate nonlinearities: Selection, uncertainty, projections, and damages. *Environmental Research Letters*, 17(8), 084025. https://doi.org/10.1088/1748-9326/ac8238

Clark, P. U., Shakun, J. D., Marcott, S. A., Mix, A. C., Eby, M., Kulp, S., et al. (2016). Consequences of twenty-first-century policy for multi-millennial climate and sea-level change. *Nature Climate Change*, 6(4), 360–369. https://doi.org/10.1038/nclimate2923

Cooper, V. T., Armour, K. C., Hakim, G. J., Tierney, J. E., Osman, M. B., Proistosescu, C., et al. (2024). Last Glacial Maximum pattern effects reduce climate sensitivity estimates. *Science Advances*, 10(16), eadk9461. https://doi.org/10.1126/sciadv.adk9461

Elderfield, H., Ferretti, P., Greaves, M., Crowhurst, S., McCave, I. N., Hodell, D., & Piotrowski, A. M. (2012). Evolution of ocean temperature and ice volume through the mid-pleistocene climate transition. *Science*, 337(6095), 704–709. https://doi.org/10.1126/science.1221294

Forster, P., Storelvmo, T., Armour, K., Collins, W., Dufresne, J.-L., Frame, D., et al. (2021). The Earth's energy budget, climate feedbacks, and climate sensitivity. In V. Masson-Delmotte, P. Zhai, A. Pirani, S. L. Connors, C. Péan, S. Berger, et al. (Eds.), *Climate change 2021: The physical science basis. Contribution of working group I to the Sixth assessment Report of the intergovernmental panel on climate change*. Cambridge, United Kingdom and New York, NY, USA. Cambridge University Press. https://doi.org/10.1017/9781009157896.009

Forster, P. M. , Richardson, T., Maycock, A. C., Smith, C. J., Samset, B. H., Myhre, G., et al. (2016). Recommendations for diagnosing effective radiative forcing from climate models for CMIP6. *Journal of Geophysical Research: Atmospheres*, 121(20), 12460–12475. https://doi.org/10.1002/2016jd025320

Fyke, J., Sergienko, O., Löfverström, M., Price, S., & Lenaerts, J. T. M. (2018). An overview of interactions and feedbacks between ice sheets and the earth system. *Reviews of Geophysics*, 56(2), 361–408. https://doi.org/10.1029/2018rg000600

Golledge, N. R., Keller, E. D., Gomez, N., Naughten, K. A., Bernales, J., Trusel, L. D., & Edwards, T. L. (2019). Global environmental consequences of twenty-first-century ice-sheet melt. *Nature*, 566(7742), 65–72. https://doi.org/10.1038/s41586-019-0889-9

Goodwin, P. (2018). On the time evolution of climate sensitivity and future warming. *Earth's Future*, 6(9), 1336–1348. https://doi.org/10.1029/2018ef000889

Hansen, J., Sato, M., Kharecha, P., Beerling, D., Berner, R., Masson-Delmotte, V., et al. (2008). Target atmospheric CO2: Where should humanity aim? *The Open Atmospheric Science Journal*, 2, 217–231. https://doi.org/10.48550/arXiv.0804.1126

Kaufman, D., McKay, N., Routson, C., Erb, M., Dätwyler, C., Sommer, P. S., et al. (2020). Holocene global mean surface temperature, a multi-method reconstruction approach. *Scientific Data*, 7(1), 201. https://doi.org/10.1038/s41597-020-0530-7

Knutti, R., & Rugenstein, M. A. A. (2015). Feedbacks, climate sensitivity and the limits of linear models. *Philosophical Transactions of the Royal Society A: Mathematical, Physical & Engineering Sciences*, 373(2054), 20150146. https://doi.org/10.1098/rsta.2015.0146

Knutti, R., Rugenstein, M. A. A., & Hegerl, G. C. (2017). Beyond equilibrium climate sensitivity. *Nature Geoscience*, 10(10), 727–736. https://doi.org/10.1038/ngeo3017

Köhler, P., Nehrbass-Ahles, C., Schmitt, J., Stocker, T. F., & Fischer, H. (2017). A 156 kyr smoothed history of the atmospheric greenhouse gases CO2, CH4, and N2O and their radiative forcing. *Earth System Science Data*, *9*(1), 363–387. https://doi.org/10.5194/essd-9-363-2017

Lambeck, K., Rouby, H., Purcell, A., Sun, Y., & Sambridge, M. (2014). Sea level and global ice volumes from the last glacial maximum to the Holocene. *Proceedings of the National Academy of Sciences*, *111*(43), 15296–15303. https://doi.org/10.1073/pnas.1411762111

Lambert, F., Bigler, M., Steffensen, J. P., Hutterli, M., & Fischer, H. (2012). Centennial mineral dust variability in high-resolution ice core data from Dome C, Antarctica. *Climate of the Past*, *8*(2), 609–623. https://doi.org/10.5194/cp-8-609-2012

Lecavalier, B. S., Milne, G. A., Simpson, M. J., Wake, L., Huybrechts, P., Tarasov, L., et al. (2014). A model of Greenland ice sheet deglaciation constrained by observations of relative sea level and ice extent. *Quaternary Science Reviews*, *102*, 54–84. https://doi.org/10.1016/j.quascirev.2014.07.018

Lenton, T. M., Williamson, M. S., Edwards, N. R., Marsh, R., Price, A. R., Ridgwell, A. J., et al. (2006). Millennial timescale carbon cycle and climate change in an efficient Earth system model. *Climate Dynamics*, *26*(7), 687–711. https://doi.org/10.1007/s00382-006-0109-9

Lisiecki, L. E. (2010). Links between eccentricity forcing and the 100,000-year glacial cycle. *Nature Geoscience*, *3*(5), 349–352. https://doi.org/10.1038/ngeo828

Lunt, D. J., Haywood, A. M., Schmidt, G. A., Salzmann, U., Valdes, P. J., & Dowsett, H. J. (2010). Earth system sensitivity inferred from Pliocene modelling and data. *Nature Geoscience*, *3*(1), 60–64. https://doi.org/10.1038/ngeo706

Madsen, M. S., Yang, S., Aðalgeirsdóttir, G., Svendsen, S. H., Rodehacke, C. B., & Ringgaard, I. M. (2022). The role of an interactive Greenland ice sheet in the coupled climate-ice sheet model EC-Earth-PISM. *Climate Dynamics*, *59*(3), 1189–1211. https://doi.org/10.1007/s00382-022-06184-6

Osman, M. B., Tierney, J. E., Zhu, J., Tardif, R., Hakim, G. J., King, J., & Poulsen, C. J. (2021). Globally resolved surface temperatures since the last glacial maximum. *Nature*, *599*(7884), 239–244. https://doi.org/10.1038/s41586-021-03984-4

Quiquet, A., Roche, D. M., Dumas, C., Bouttes, N., & Lhardy, F. (2021). Climate and ice sheet evolutions from the last glacial maximum to the pre-industrial period with an ice-sheet–climate coupled model. *Climate of the Past*, *17*(5), 2179–2199. https://doi.org/10.5194/cp-17-2179-2021

Rial, J. A., Oh, J., & Reischmann, E. (2013). Synchronization of the climate system to eccentricity forcing and the 100,000-year problem. *Nature Geoscience*, *6*(4), 289–293. https://doi.org/10.1038/ngeo1756

Rohling, E. J., Marino, G., Foster, G. L., Goodwin, P. A., von der Heydt, A. S., & Köhler, P. (2018). Comparing climate sensitivity, past and present. *Annual Review of Marine Science*, *10*(1), 261–288. https://doi.org/10.1146/annurev-marine-121916-063242

Rohling, E. J., Medina-Elizalde, M., Shepherd, J. G., Siddall, M., & Stanford, J. D. (2012). Sea surface and high-latitude temperature sensitivity to radiative forcing of climate over several glacial cycles. *Journal of Climate*, *25*(5), 1635–1656. https://doi.org/10.1175/2011jcli4078.1

Rohling, E. J., Sluijs, A., Dijkstra, H. A., Köhler, P., van de Wal, R. S. W., von der Heydt, A. S., et al. (2012). Making sense of palaeoclimate sensitivity. *Nature*, *491*(7426), 683–691. https://doi.org/10.1038/nature11574

Rohling, E. J., Yu, J., Heslop, D., Foster, G. L., Opdyke, B., & Roberts, A. P. (2021). Sea level and deep-sea temperature reconstructions suggest quasi-stable states and critical transitions over the past 40 million years. *Science Advances*, *7*(26), eabf5326. https://doi.org/10.1126/sciadv.abf5326

Ryan, J. C., Smith, L. C., van As, D., Cooley, S. W., Cooper, M. G., Pitcher, L. H., & Hubbard, A. (2019). Greenland Ice Sheet surface melt amplified by snowline migration and bare ice exposure. *Science Advances*, *5*(3), eaav3738. https://doi.org/10.1126/sciadv.aav3738

Schmidt, G. A., Romanou, A., Roach, L. A., Mankoff, K. D., Li, Q., Rye, C. D., et al. (2023). Anomalous meltwater from ice sheets and ice shelves is a historical forcing. *Geophysical Research Letters*, *50*(24), e2023GL106530. https://doi.org/10.1029/2023gl106530

Shackleton, S., Seltzer, A., Baggenstos, D., & Lisiecki, L. E. (2023). Benthic δ18O records Earth's energy imbalance. *Nature Geoscience*, *16*(9), 797–802. https://doi.org/10.1038/s41561-023-01250-y

Shakun, J. D., Lea, D. W., Lisiecki, L. E., & Raymo, M. E. (2015). An 800-kyr record of global surface ocean δ18O and implications for ice volume-temperature coupling. *Earth and Planetary Science Letters*, *426*, 58–68. https://doi.org/10.1016/j.epsl.2015.05.042

Simms, A. R., Lisiecki, L., Gebbie, G., Whitehouse, P. L., & Clark, J. F. (2019). Balancing the last glacial maximum (LGM) sea-level budget. *Quaternary Science Reviews*, *205*, 143–153. https://doi.org/10.1016/j.quascirev.2018.12.018

Smith, C. J., Kramer, R. J., Myhre, G., Alterskjær, K., Collins, W., Sima, A., et al. (2020). Effective radiative forcing and adjustments in CMIP6 models. *Atmospheric Chemistry and Physics*, *20*(16), 9591–9618. https://doi.org/10.5194/acp-20-9591-2020

Smith, R. S., George, S., & Gregory, J. M. (2021). FAMOUS version xotzt (FAMOUS-ice): A general circulation model (GCM) capable of energy- and water-conserving coupling to an ice sheet model. *Geoscientific Model Development*, *14*(9), 5769–5787. https://doi.org/10.5194/gmd-14-5769-2021

Snyder, C. W. (2016). Evolution of global temperature over the past two million years. *Nature*, *538*(7624), 226–228. https://doi.org/10.1038/nature19798

Spencer, R. W., & Christy, J. R. (2023). Effective climate sensitivity distributions from a 1D model of global ocean and land temperature trends, 1970–2021. *Theoretical and Applied Climatology*, *155*(1), 299–308. https://doi.org/10.1007/s00704-023-04634-7

Stone, E. J., & Lunt, D. J. (2013). The role of vegetation feedbacks on Greenland glaciation. *Climate Dynamics*, *40*(11), 2671–2686. https://doi.org/10.1007/s00382-012-1390-4

Vizcaíno, M., Mikolajewicz, U., Gröger, M., Maier-Reimer, E., Schurgers, G., & Winguth, A. M. E. (2008). Long-term ice sheet–climate interactions under anthropogenic greenhouse forcing simulated with a complex Earth System Model. *Climate Dynamics*, *31*(6), 665–690. https://doi.org/10.1007/s00382-008-0369-7

Willeit, M., Ganopolski, A., Dalmonech, D., Foley, A. M., & Feulner, G. (2014). Time-scale and state dependence of the carbon-cycle feedback to climate. *Climate Dynamics*, *42*(7), 1699–1713. https://doi.org/10.1007/s00382-014-2102-z

Zeebe, R. E. (2013). Time-dependent climate sensitivity and the legacy of anthropogenic greenhouse gas emissions. *Proceedings of the National Academy of Sciences*, *110*(34), 13739–13744. https://doi.org/10.1073/pnas.1222843110

Zhu, J., & Poulsen, C. J. (2021). Last Glacial Maximum (LGM) climate forcing and ocean dynamical feedback and their implications for estimating climate sensitivity. *Climate of the Past*, *17*(1), 253–267. https://doi.org/10.5194/cp-17-253-2021